Sustainable purification of phosphoric acid contaminated with Cr(VI) by Ag/Ag3PO4 coated activated carbon/montmorillonite under UV and solar light: Materials design and photocatalytic mechanism

Sustainable purification of phosphoric acid contaminated with Cr(VI) by Ag/Ag_3PO_4 coated activated carbon/montmorillonite under UV and solar light: materials design and photocatalytic mechanistic

Nesrine Abderrahim[1], Claudia L. Bianchi[2] , Hédi Ben Amor[1], Imen Fellah[1], Alessia Giordana[3], Giuseppina Cerrato[3], Ridha Djellabi[2,]*

[1]Engineering school (ENIG), RL Processes, Energetic, Environment and ElectricSystems (PEESE) University of Gabes. Gabes 6072, Tunisia.

[2]Department of Chemistry, University of Milan, Via Golgi 19, Milano 20133, Italy

[3]Department of Chemistry, University of Turin, Via Pietro Giuria 7, 10125 Turin, Italy

Corrosponding author: Ridha Djellabi (ridha.djellabi@yahoo.com)

Graphical abstract

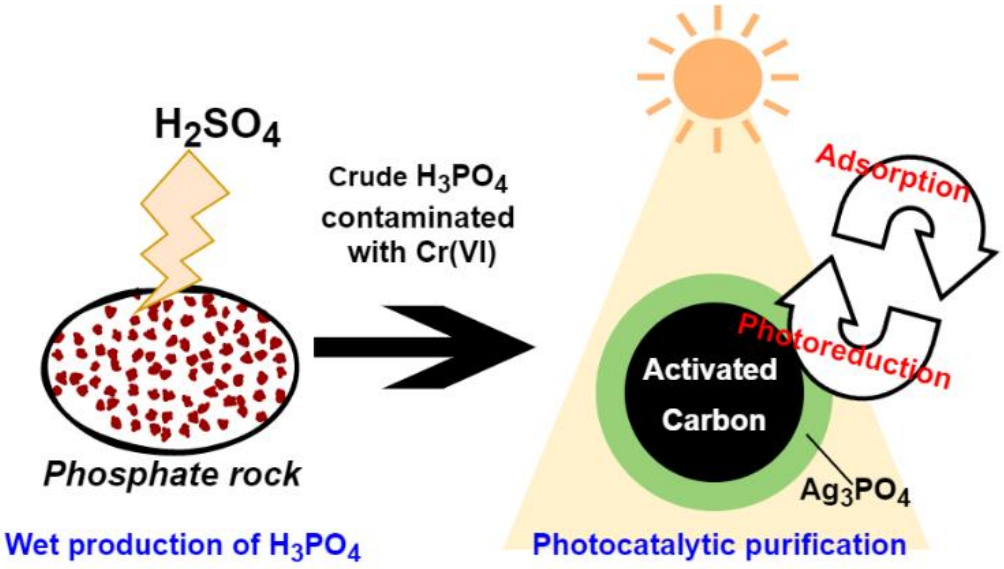

Highlights

- Investigate the purification of phosphoric acid via photocatalytic technology
- Design of highly synergistic visible light photoactive Ag_3PO_4-adsorbent composites
- Comparative efficiency of type of adsorbent supports for Ag_3PO_4 particles
- Comparative photoreduction of Cr(VI) in aqueous and phosphoric acid solutions
- Role of hole scavenger molecule in in aqueous and phosphoric acid solutions

Abstract,

Wet production of phosphoric acid, the most used low-cost industrial approach, first leads to an impure phosphoric acid contaminated by organic and heavy metals species. Such a crude phosphoric acid requires costly purification before its usage. The present work has investigated for the first time the recovery of Cr(VI), as one of the most co-existed heavy metals, from the phosphoric acid medium. For this purpose, three composites based on Ag_3PO_4 coated on Montmorillonite (MAg_3PO_4), commercial activated carbon ($ACAg_3PO_4$), and synthetic activated carbon obtained from agricultural biomass ($SACAg_3PO_4$). The photocatalytic reduction of Cr(VI) was studied comparatively in the absence and presence of citric acid as a hole scavenger under UV and solar light irradiations. Under UV light, MAg_3PO_4 was the most efficient, while activated carbon-based photocatalysts showed higher reduction rates under solar light which might be due to the photosensitizing effect. Compared with aqueous medium, the photocatalytic reduction was very effective without citric acid in phosphoric acid medium because of the low photogeneration of reactive oxygen species (ROSs). The chemical bonds formed between Ag_3PO_4 and support materials, as proved by XPS, may enhance the photocatalytic activity as a result of enhanced charges photogeneration and separation. $SACAg_3PO_4$ showed higher reduction ability even at higher Cr(VI) concentrations (100-300 ppm). A comparison study showed that $SACAg_3PO_4$ is more effective than as-prepared $ACTiO_2$. This investigation shows promising findings to widen the application of photocatalytic technology in different industrial fields.

Keywords: Phosphoric acid purification, Photocatalytic technology, Cr(VI) recovery, Ag_3PO_4 coating; Biomass valorisation.

1. Introduction

The purification of crude phosphoric acid by removing metallic and organic contaminants has a great importance due to its huge applications in different fields such as petrochemistry, alimentary industry, agriculture, detergents production and pharmaceutical industry (Bahrpaima 2017; Ma et al. 2013; BAI and ZENG 2006). Highly purified H_3PO_4 is often manufactured through two basic common technologies such as thermal (Ma et al. 2013) and wet approaches. In the thermal process, H_3PO_4 is produced via the use of water or/and diluted phosphoric acid to absorb P_4O_{10} from phosphate rocks via burning in an oxygenated environment. The thermal process is very effective in producing high-quality H_3PO_4; however, due to the huge energy requirement, it has been abandoned in most European countries (Association 2000). While some Asian countries. e.g., China or Kazakhstan, are still using this process to produce H_3PO_4. Around 95% of produced H_3PO_4 in European countries and the rest of the world is carried out via the economic wet process, which focuses mainly on the attack of phosphate rock with H_2SO_4, even it is accompanied by the co-production of many toxic impurities, e.g., heavy metals, fluoride, and phosphogypsum (one of the common toxic contaminates in phosphoric acid produced by wet process (Association 2000)). Therefore, further purification of produced phosphoric acid is required to decrease the concentration of different impurities to acceptable regulatory levels (Belboom, Szöcs, and Léonard 2015; Kouzbour et al. 2019). One of the common approaches to remove metallic or/and organic impurities from at large scale is liquid-liquid extraction (Kijkowska et al. 2002; Chuanpin and Gusheng 2003; Boulkroune and Meniai 2012; Wu et al. 2018), crystallization (Chen et al. 2013), membrane (Zhong et al. 2021; Khaless et al. 2021; ZHANG et al. 2016), adsorption (El-Asmy et al. 2008; El-Zahhar, El-Deen, and Sheha 2013), nanofiltration (Diallo et al. 2013), electrooxidation (Nasr et al. 2005), ion-exchange (Tang et al. 2018; Amin 2020).

Photocatalytic technology is able to oxidize most of the organic pollutants via the photogeneration of reactive oxygen species (ROSs) under light irradiation. In addition, such a process can perfectly

reduce heavy metals by the photogenerated electrons on the conduction band, followed by their deposition on the surface. Photocatalysis towards water purification has passed through a long path, however, due to several technology issues, its transfer to real-world application is still very rare (Alalm et al. 2021; Loeb et al. 2018). The transfer of photocatalytic technology to real use could be achieved through different ways such as finding solutions to unsolved environmental problems, developing highly competitive or/and economic photocatalytic technologies, or unique application as discussed recently by Djellabi et al. (Djellabi, Giannantonio, et al. 2021). In this work, for the first time, photocatalytic technology was employed for the purification of crude phosphoric acid. In this context, three types of adsorbent/semiconductor composites were fabricated, including Ag_3PO_4-Montmorillonite, Ag_3PO_4-commercial activated carbon, and Ag_3PO_4-synthetic activated carbon. Ag_3PO_4 has shown excellent photocatalytic activity and enhanced visible-light response (bandgap of 2.43 eV) (Naciri et al. 2021; Trench et al. 2018). In photocatalytic materials, it was proved through long fundamental scientific research that the naked (or single) photocatalysts show several drawbacks such as low surface area, high generation of by-products, less mass transfer, and so on. Several surface/structure modifications and combinations have been suggested to counterbalance these issues. One of the most successful approaches to enhance the photocatalytic ability and to solve some technological issues is the combination of inorganic semiconductors with highly supportive porous materials. In such a process, adsorption and photocatalysis work cooperatively in a continuous way to oxidize/reduce water pollutants synergistically through the so-called Adsorb & Shuttle process (Djellabi et al. 2020; Saber et al. 2021). Since crude phosphoric acid exhibits a huge amount of hexavalent chromium, which needs further purification, herein, the photocatalytic reduction of Cr(VI) was investigated comparatively under UV and solar light in both water and phosphoric acid mediums. The mechanistic pathways during the photocatalytic reduction in different mediums were discussed. The photocatalytic efficiency at very high Cr(VI) concentrations (200-300 ppm) in a phosphoric acid medium (that is similar to real cases) was performed.

2. Materials and methods

2.1. Synthesis and characterization of Ag_3PO_4 coated materials

Three materials were used as support for Ag_3PO_4, including montmorillonite (M), commercial activated carbon (AC), and synthetic activated carbon (SAC). The coating of these materials was carried out by direct precipitation of Ag_3PO_4 on the surface. For this purpose, 1 g of the support (M, AC, or SAC) and 25 mL of deionized water are sonicated for 20 min. Then under stirring, 5 mL of $AgNO_3$ (0.6 M) is added dropwise and left for 1 h. 5 mL of NaH_2PO_4 (0.2 M) is added dropwise under vigorous stirring, and the mixture was left under stirring for 2 h at 60°C. The resultant solid was washed by ultrapure water and dried for a night at 120°C. Figure 1 shows the images of as-prepared photocatalysts before and after Ag_3PO_4 coating.

The materials were characterized by Fourier transform infrared spectroscopy analyses (FT-IR) analysis using a Bruker Vertex 70 spectrophotometer (Bruker, Billerica, MA, US). XRD spectra of samples were recorded on a PANalytical X'PERT-PRO diffractometer with monochromatic CuKα radiation (λ = 1.54056 Å). X-ray photoelectron spectra (XPS) were recorded on a XPS PHI Quantum instrument.

Diffused reflectance spectra were measured with a Cary 5000 UV-Vis spectrophotometer (Agilent Technology). The Tauc plot was obtained and employed to evaluate the bandgap value of synthesized materials. Therefore, the evaluation of the bandgap value was obtained by plotting $[F(R)hv]1m\diagup$ versus hv as according to the equation $[F(R)hv]1/m= K(hv-Eg)$. In which $F(R)$ is the Kubelka-Munk function, K is a constant characteristic of the material, hv is the energy of incident photons and Eg is the bandgap. The value of m depends on the type of transition and represents m=1/2 for direct and m=2 for indirect allowed transitions.

Figure 1. Images of materials before and after coating with Ag_3PO_4.

2.2. Photocatalytic tests

The as-prepared photocatalysts were tested for the removal of Cr(VI) from aqueous and phosphoric acid solutions under UV and solar light. UVA lamp (500W, Jelosil, Vomodrone, Italy) at 0.1 mW/m^2 and solar lamp (35 $W \cdot m^{-2}$, ULTRA VITALUX 300 W-OSRAM, OSRAM, Múnich, Germany) were used. A desired amount of photocatalyst is added to a volume of Cr(VI) solution in water or phosphoric acid medium to carry out the photocatalytic experiments. The phosphoric acid solution was prepared by synthetic phosphoric acid and water (52 % P_2O_5). The Cr(VI) solution is exposed to light irradiation, and samples were taken at different intervals for Cr(VI) analysis using 1,5-Diphenylcarbazide at 540 nm via UV/Vis spectrophotometry (Djellabi, Zhang, et al. 2019).

3. Results and discussion

3.1. Characterization

Figure 2 shows the XRD spectra of bare Ag_3PO_4, MAg_3PO_4, $ACAg_3PO_4$, and $SACAg_3PO_4$ samples. Ag_3PO_4 pattern shows diffraction peaks which perfectly indicate the body-centered cubic structure of Ag_3PO_4 (Inorganic Crystal Structure Database (ICSD) No. 14000) (Botelho et al. 2015). Similarly, body-centered cubic structure diffraction peaks of Ag_3PO_4 appeared in MAg_3PO_4, $ACAg_3PO_4$, and $SACAg_3PO_4$ samples as well. It can be noticed that the main diffraction peak (211) at 2θ: 33.3◦ is

more intense in terms of $ACAg_3PO_4$ compared to MAg_3PO_4 and $SACAg_3PO_4$ samples. The nature of commercial activated carbon surface might boost the high crystallization of Ag_3PO_4. Apart from diffraction peaks of Ag_3PO_4, as indicated in **Figure 2** with green spheres, planes of the face-centered cubic structure of metallic Ag were appeared at 2θ: 38.3, 44.5, 64.6, and 77.9° (JCPDS no-65–2871) in both $ACAg_3PO_4$ and $SACAg_3PO_4$ (Wan et al. 2015). The co-presence of metallic Ag and Ag_3PO_4 may influence the light absorption, redox charges generation and separation.

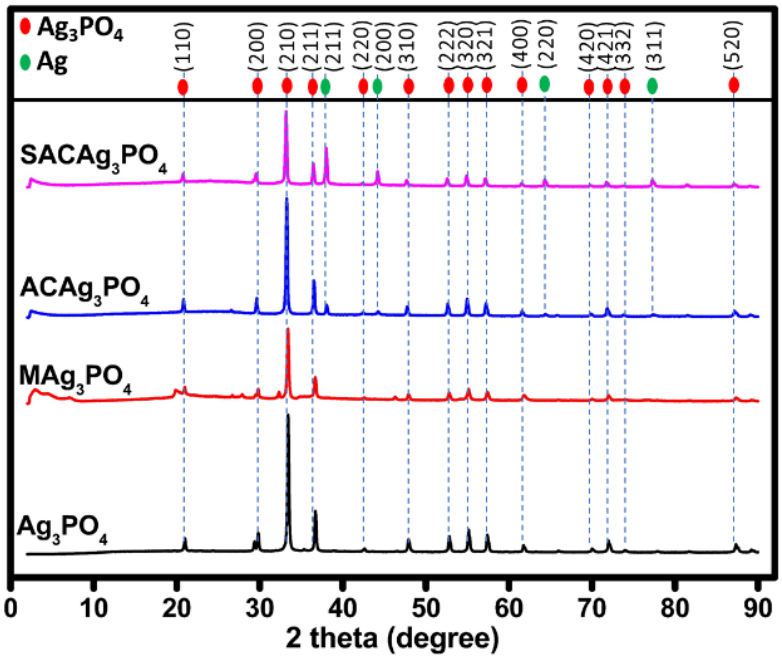

Figure 2. XRD spectra of Ag_3PO_4, MAg_3PO_4, $ACAg_3PO_4$ and $SACAg_3PO_4$.

Figure 3 shows FTIR curves of bare Ag_3PO_4 and Ag_3PO_4 coated materials. Bare Ag_3PO_4 shows a main characteristic peak centered at around 1010 cm^{-1} due to the asymmetric vibration of P-O-P bands in PO_4^{3-} (Abroushan, Farhadi, and Zabardasti 2017). The small peak at around 884 cm^{-1} is assigned to symmetric vibration of P-O-P bands. The peak appeared at 560 cm^{-1} is due to the OP–O bending vibration (Ma et al. 2016). It was produced a sharp band at 1420 $cm^{-1,}$ which might be attributed to phosphoryl P=O bonds in PO_4^{3-} (Zhou et al. 2016). Pure Montmorillonite shows a large band lies at 950-1100 cm^{-1} that is assigned to the characteristic Si-O stretching (Saber et al. 2021). Several peaks at 800, 785, and 700 cm^{-1} are associated with Si-O stretching mode. While peaks at around 915, 880, and near 840 cm^{-1} are due to AlAlOH, AlFeOH, and AlMgOH deformations,

respectively (Ahmed et al. 2018; Kloprogge 2017). The peak at 600 cm^{-1} might be due to a combination of Al-O-Si deformation and Si-O-Si deformation, while the peak at 540 cm^{-1} refers to Si-O bending. In terms of MAg_3PO_4, the band at around 1000 cm^{-1} turns stronger as a result of the combination of P-O-P asymmetric vibration of P-O-P of Ag_3PO_4 and Si-O stretching of the montmorillonite. Similarly, the intensity of peak at around 540 cm^{-1} was enhanced due to combination of OP–O bending vibration and Si-O bending. 1420 cm^{-1}, which could be attributed to the peak phosphoryl P=O bonds. Regarding activated carbon samples (**Figure 3.b**), after the coating of Ag_3PO_4 on both AC and SAC, the intense peak of asymmetric vibration of P-O-P bands was produced. The large band centered at around 3400 cm^{-1} is attributed to OH^- vibration.

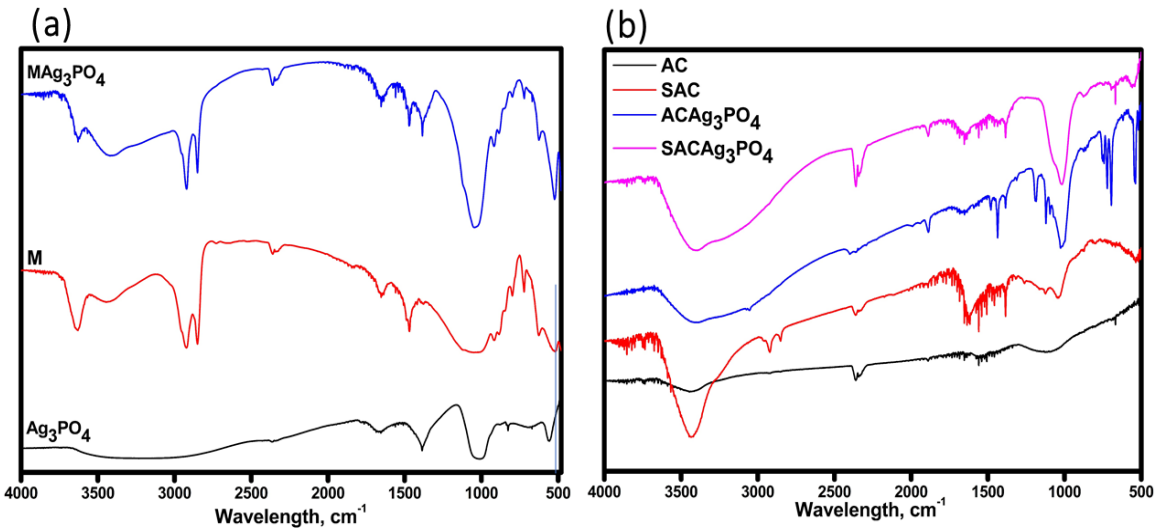

Figure 3. FTIR curves of (a) Ag_3PO_4, M, and MAg_3PO_4, and (b): AC, SAC, $ACAg_3PO_4$ and $SACAg_3PO_4$.

Figure 4 shows XPS survey spectra of Ag_3PO_4, MAg_3PO_4, $ACAg_3PO_4$, and $SACAg_3PO_4$ samples, and high-resolution XPS spectra of Ag 3d, P 2P, O 1s, and C 1s. Compared to bare Ag_3PO_4, Ag 3d high-resolution XPS profiles of samples show a clear shift towards higher binding energies. The peak shifting was calculated to be 1.2, 1.3, and 0.4 eV for MAg_3PO_4, $ACAg_3PO_4$, and $SACAg_3PO_4$ samples, respectively. It is important to point out that the sifting in XPS peaks is due to the change in oxidation states of elements as well as it depends on the interface interactions and local chemical environment, in other words, the chemical nature of neighboring atoms (Chastain and King Jr 1992). In general, if

the electronegativity of the neighboring atom is higher than that of the analyzed element, a positive shift is obtained while the reserve is true. The deconvoluted Ag 3d peaks (Ag $3d_{5/2}$ and Ag $3d_{3/2}$) were divided into two peaks for all samples, which are assigned to Ag^{+} and $Ag^{(0)}$ (Bianchi et al. 2020). As above-discussed, Ag 3d peaks shifting is due to the in situ formation of Ag(0) and the surface interaction of $Ag^{(+)}$ with neighboring atoms (i.e., C, O…etc) on the surface of material supports. The formation of metallic silver nanoparticles was already confirmed by XRD analysis in the cases of $ACAg_3PO_4$ and $SACAg_3PO_4$. The XPS profiles of P 2P exhibit one peak at around 133.4 eV which is due to the phosphorus in Ag_3PO_4. This peak was shifted to higher binding energy in MAg_3PO_4, $ACAg_3PO_4$, and $SACAg_3PO_4$ samples due to the surface interactions. The high-resolution of C 1s exhibits three main deconvoluted peaks associated with C-C sp2, C-C sp3, C-O (Djellabi, Yang, Xiao, et al. 2019). However, C 1s spectrum of $SACAg_3PO_4$ exhibits an additional fourth strong peak due to C=O or oxygen bridging atoms (Djellabi, Yang, Wang, et al. 2019). The high-resolution O 1s profile of Ag_3PO_4 was split into three peaks at around 529.8, 531.4, and 533 eV, which are associated with lattice oxygen, O^{2-} in Ag_3PO_4 and OH^{-} groups from adsorbed water, respectively. In terms of MAg_3PO_4, $ACAg_3PO_4$ samples, the three peaks were also produced along with a change in their intensities and a strong shift towards higher binding energies. In the case of $SACAg_3PO_4$, a fourth strong peak was produced, which could be allotted to the bridging oxygen (Ag-O-C). C 1s spectrum of $SACAg_3PO_4$ shows as well an additional peak, suggestiong the formation of Ag-O-C bonds. The significant shifting in peaks indeed reveals a strong interaction between material supports (M, AC, and SAC) and Ag_3PO_4 in the heterojunction system.

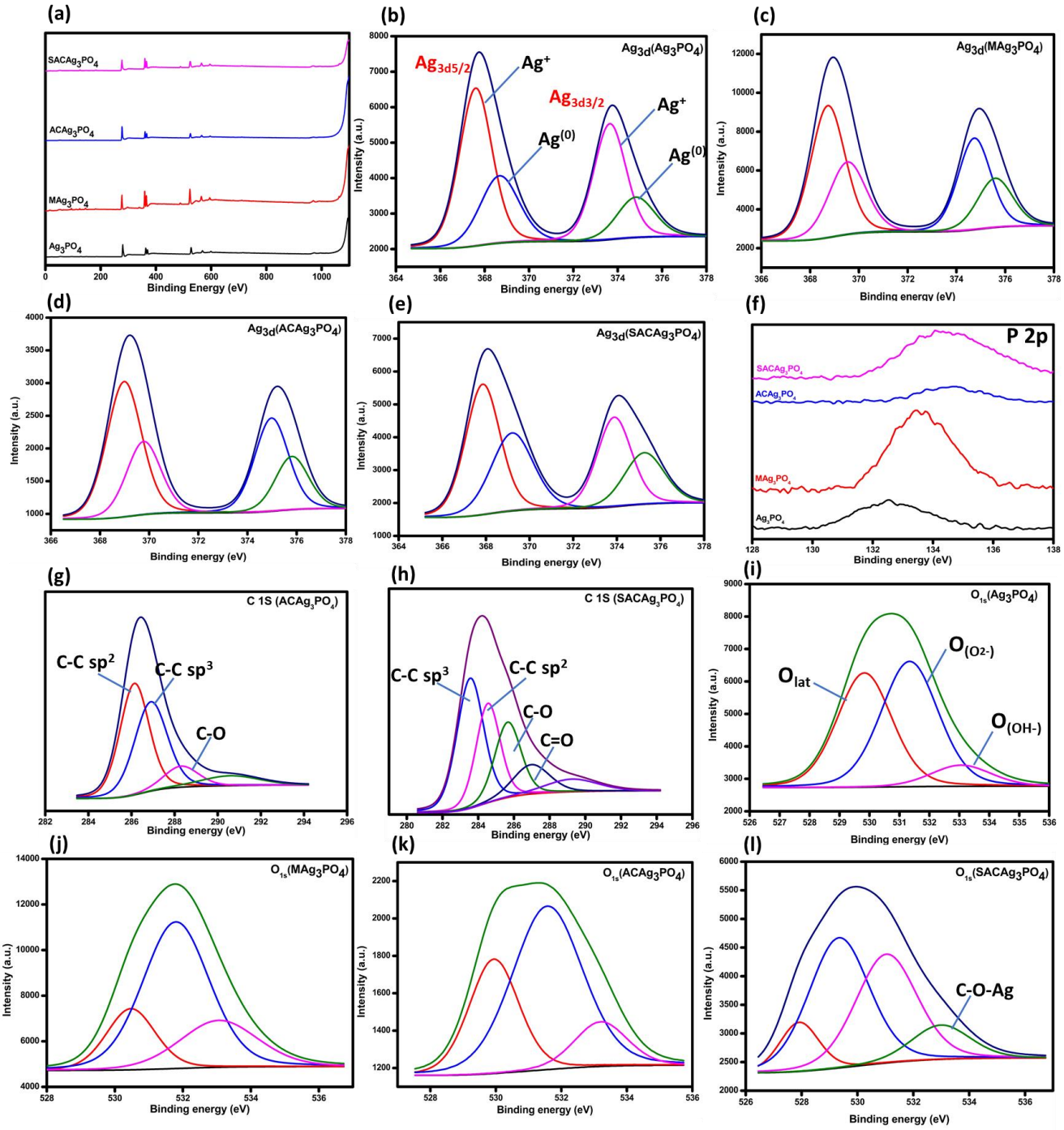

Figure 4. (a): XPS survey of Ag_3PO_4, MAg_3PO_4, $ACAg_3PO_4$, and SAC Ag_3PO_4. Deconvoluted Ag 3d peaks (Ag $3d_{5/2}$ and Ag $3d_{3/2}$) for **(b)**: Ag_3PO_4, **(c)**: MAg_3PO_4, **(d)**: $ACAg_3PO_4$ and **(e)**: $SACAg_3PO_4$. **(f)**: P 2p spectra of all samples. **(g)** Deconvolved C1S peaks of $ACAg_3PO_4$. **(h)** Deconvolved C1S peaks of $SACAg_3PO_4$. Deconvolved O_{1S} peaks of **(i)**: Ag_3PO_4, **(j)**: MAg_3PO_4, **(k)**: $ACAg_3PO_4$, and **(l)**: $SACAg_3PO_4$.

The results of UVDRS analysis are shown in **Figure 5**. It can be seen from the spectra of absorbance of samples (**Figure 5.a**) that a better visible light responsive can be found in MAg_3PO_4, $ACAg_3PO_4$ and $SACAg_3PO_4$ absorption edges compared to bare Ag_3PO_4. As observed by XPS and XRD, a band testifying the presence of AgNPs at 452 nm (Bianchi et al. 2020) was produced in all samples. **Figure 5.b** shows the normalized K-M curves in order to calculate the band gaps, and permits to enhance similarity and difference between samples. In terms of Ag_3PO_4, the band gap for indirect (m=2) and direct transition (m=1/2) were found to be 2.45 eV and 2.55 eV, respectively, slightly higher than literature values (2.36-2.46 eV) (Naciri et al. 2021). The calculation of band gap in $ACAg_3PO_4$ sample is uncertain due to the high noise in the derivatives, that could be related to the high absorbance of these samples. However, the band gap for $ACAg_3PO_4$ would be estimated to be around 2.35 eV. A red-shift can be observed also in MAg_3PO_4 absorption edge, but was not possible to calculate the band gap, for the lack of linearity.

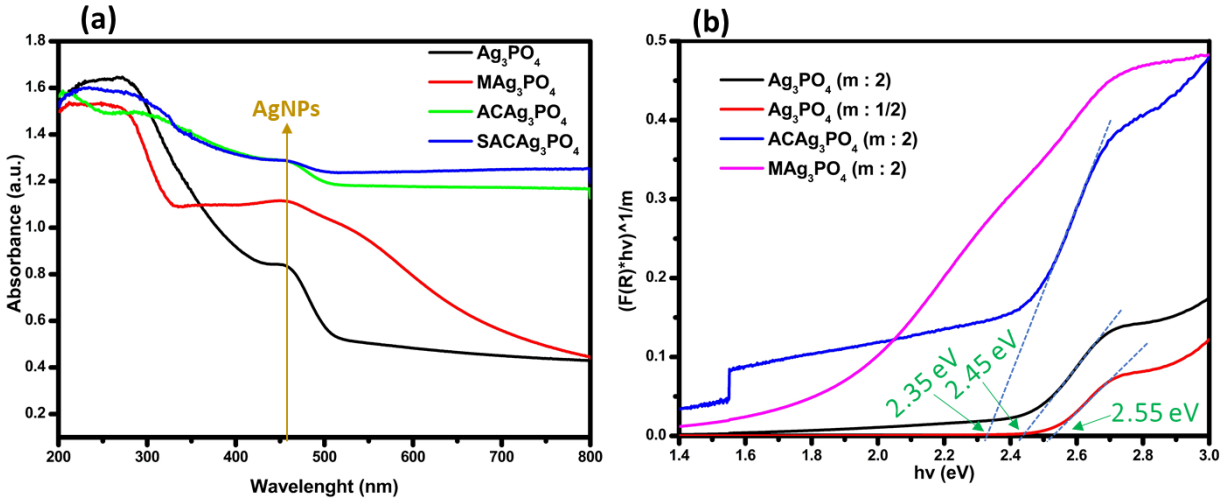

Figure 5. Absorption spectra (a) and normalized K-M curves (b) of Ag_3PO_4, MAg_3PO_4, $ACAg_3PO_4$, and SAC Ag_3PO_4 samples.

3.2. Photocatalytic reduction of Cr(VI) in aqueous solution

The adsorption and photocatalytic reduction of Cr(VI) by different materials under UV and solar light in aqueous solution are shown in **Figure 6.** Citric acid was used as a hole scavenger, and its role is basically to react with positive holes and photogenerated reactive oxygen species (ROSs) to boost the

photocatalytic reduction of Cr(VI) and avoid the re-oxidation of formed Cr(III) into Cr(VI) . However, in real wastewaters, usually organic and metallic pollutants co-exist. In terms of MAg_3PO_4 (**Figure 6.a**), MAg_3PO_4 showed enhanced dark adsorption up to around 20 % compared to bare M, which could be due to the insertion of Ag_3PO_4 into the montmorillonite interlayers leading to enhance the porosity and creating novel functional groups. MAg_3PO_4 shows around 50% reduction of Cr(VI) under UV light irradiation without the addition of citric acid. Under UV in the presence of citric acid, a total reduction was obtained within 60 min. The photocatalytic reduction under solar light was around 40 and 70% without and with citric acid, respectively. In terms of $ACAg_3PO_4$, the dark adsorption using bare AC was around 48 %, while $ACAg_3PO_4$ exhibits lower adsorption than bare AC of around 25 %. Under light irradiation, an enhanced removal as compared to dark adsorption was observed, wherein the addition of citric acid further improves the reduction under both UV and solar light irradiations. **Figure 6.c** shows that $SACAg_3PO_4$ exhibits better adsorption and photocatalytic activities than $ACAg_3PO_4$. The comparison of the photoreduction under solar light by different as-prepared materials is shown in **Figure 6.d**. It can be deduced that activated carbon-based photocatalysts exhibit the highest photoactivity compared to MAg_3PO_4, even though this latter was the most effective under UV light. Black activated carbon can enhance photoexcitation of Ag_3PO_4 and the yield of the photoproduced electrons through the photosensitizing effect at the interface of the composite. For comparison, tests with bar Ag_3PO_4 and activated carbon coated by TiO_2 were carried out to prove the high efficiency of the $SACAg_3PO_4$ system. In terms of Ag_3PO_4, the photocatalytic reduction of Cr(VI) at 50 ppm, without and with citric acid, was found to be 30 and 51 %, respectively within 2 h. While the use of $ACTiO_2$ showed a reduction rate of 77.3 % in the presence of citric acid within 2 h. The main reasons behind the increase of photoreduction rates by $SACAg_3PO_4$ compared to bare Ag_3PO_4 is the synergism in terms of adsorption and photoactivity to make the Adsorb & Shuttle process into action (Djellabi et al. 2020), wherein the sorbing domain (AC) concentrates Cr(VI) species, followed by their reduction by the photogenerated electrons coming from the photoactive environment. In addition, the charges transfer between the support (AC) and

Ag_3PO_4 through chemical bonds can enhance the separation of redox charges. AC carbon may improve the photoactivity through the photosensitizing effect. It was also noticed, by XRD and XPS, the formation of AgNPs along with Ag_3PO_4, which in turn may play the role of electron receiver/concentrator. On the other hand, $ACTiO_2$ showed lower photoreduction ability as compared to $ACAg_3PO_4$ because this latter exhibits a better photoreducing ability as a result of its more negative conduction band, and also the smaller bandgap of Ag_3PO_4.

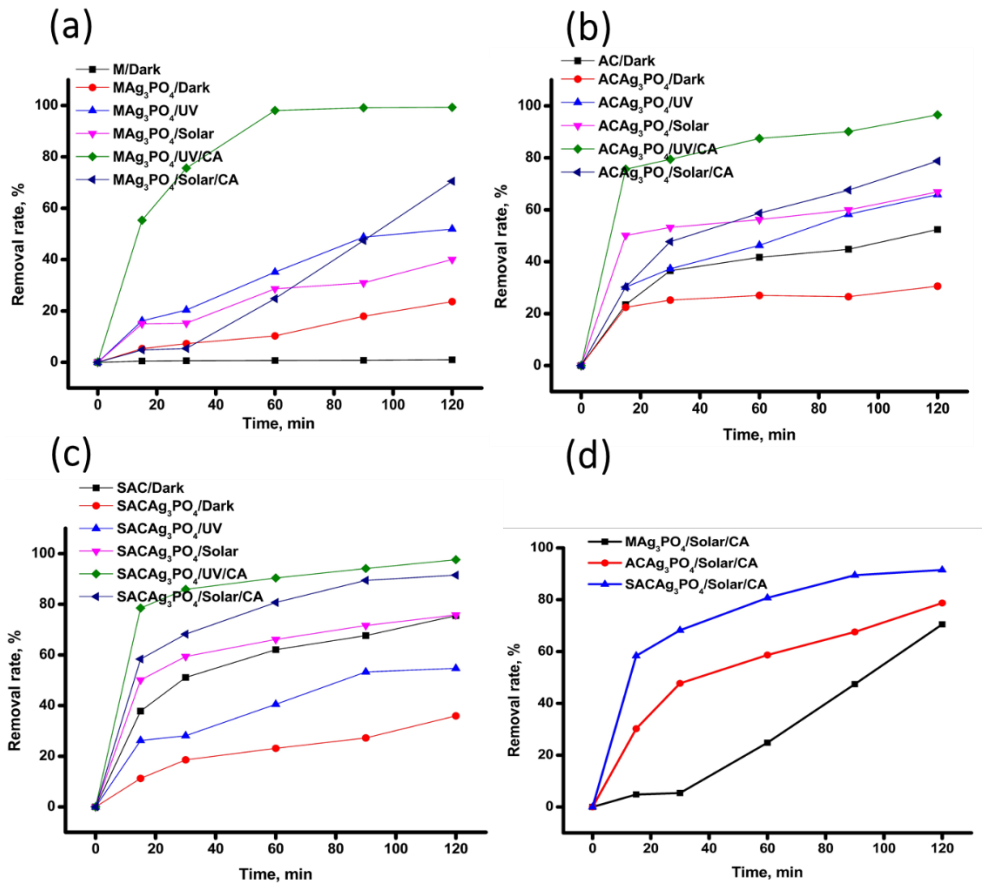

Figure 6. Adsorption and photocatalytic reduction of Cr(VI) under UV and solar light with and without citric acid by (a): MAg_3PO_4, (b): $ACAg_3PO_4$, and (C): $SACAg_3PO_4$. (d): Comparison of photocatalytic reduction of Cr(VI) in the presence of citric acid using MAg_3PO_4, $ACAg_3PO_4$, and $SACAg_3PO_4$ under solar light. [Cr(VI)]: 50 ppm, [citric acid]: 50 ppm, [Photocatalyst]: 1 g/L.

Figure 7 shows the effect of citric acid on the photocatalytic reduction of Cr(VI) at different concentrations using $SACAg_3PO_4$ under UV light. The addition of citric acid has a significant role in the photoreduction performance because of its role as a hole and ROSs scavenger. Without citric acid,

the photoreduction of Cr(VI) can take place slightly, as discussed above. Our previous works discussed the mechanistic pathways of hole scavengers in detail (Marinho et al. 2017; Djellabi, Zhao, et al. 2021; Djellabi and Ghorab 2015). Shortly, the presence of hole scavenger molecules during the photocatalytic reduction of heavy metals enhances the performance via different ways: (i): the direct oxidation of hole scavenger molecule in the valance band by positive holes helps to liberate photogenerated electrons on the conduction band for the photoreduction reaction, (ii): the reaction of hole scavenger molecule with photoproduced ROSs limits the unwanted reverse oxidation of produced Cr(III) into Cr(VI). The oxidation of hole scavenger molecules may lead to some reductive species that contribute to the photoreduction of Cr(VI).

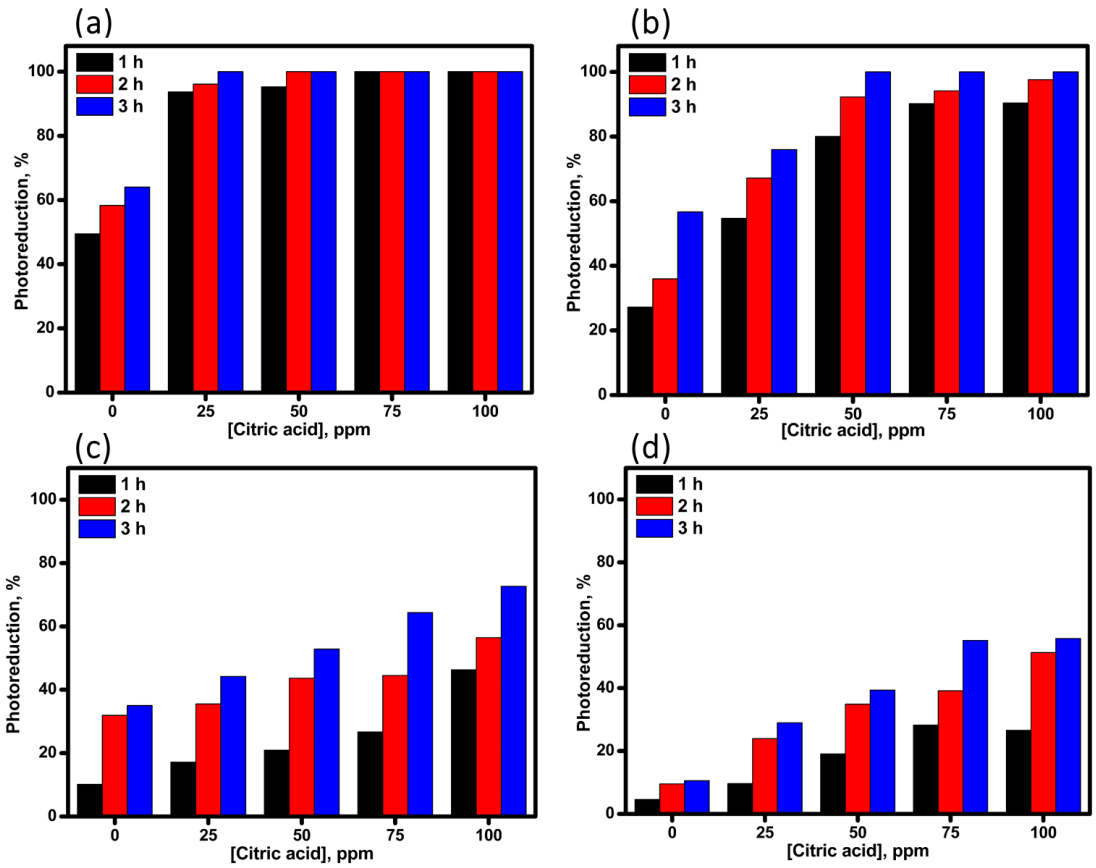

Figure 7. Effect of citric acid concentration on the photocatalytic reduction of Cr(VI) in water under UV light at different Cr(VI) concentrations (a): [Cr(VI)]: 25 ppm, (b): [Cr(VI)]: 50 ppm, (c): [Cr(VI)]: 75 ppm, (a): [Cr(VI)]: 100 ppm. pH: 2, mass of photocatalyst: 1 g/L.

3.3. Photocatalytic reduction of Cr(VI) in phosphoric acid

The photocatalytic reduction of Cr(VI) using different as-prepared photocatalysts (MAg_3PO_4, $ACAg_3PO_4$, and $SACAg_3PO_4$) in the phosphoric acid medium was investigated without the addition of citric acid under UV light (**Figure 8.a**). It can be observed that the reduction ability in phosphoric acid medium is very fast even without the presence of citric acid, compared with the results obtained in water medium under the same conditions ([Cr(VI]: 50 ppm). To confirm that the fast reduction is not due to the pH of aqueous solution (pH: 2) and phosphoric acid (1.2), a control experiment in aqueous solution at pH 1.2 (data now shown) was carried out, and it was observed that the photoreduction at pH 2 and 1.2 are similar after 3 h. Therefore, it may be deduced from these results that the photocatalytic reduction in phosphoric acid is much faster than that in water medium. In fact, the generation of reactive oxygen species in phosphoric acid could be lesser as compared with water medium, which limits the unwanted re-oxidation of Cr(III). These results are very interesting in terms of technology towards the application of photocatalysis system for the recovery of heavy metals from crude phosphoric acid, as there is no need to add hole scavenger molecules to the medium. To further evaluate the photocatalytic performance of $SACAg_3PO_4$/UV, experiments with higher Cr(VI) concentrations of 100, 200, and 300 ppm were carried out, and the results are shown in **Figures 8, c,b,d,** respectively. It can be seen that, at Cr(VI) of 100 ppm, a total reduction can be found with and without the addition of citric acid within 3 h. At 200 ppm, the total reduction within 3 h was slightly lower in the experiment that performed without citric acid. At 300 ppm, the role of citric acid was evident. The high yield of Cr(VI) may block the surface of $SACAg_3PO_4$ which requires the catalysis of the reaction using hole scavenger molecules. In general, crude phosphoric acid contains organic pollutants, which might play the role of hole scavenger during the photoreduction of Cr(VI). As shown in **Figure 9**, the combination of Ag/Ag_3PO_4 on the surface of activated carbon results in excellent photocatalytic ability because of synergitem in terms of electrons generation and separation. The photogenerated electrons of the conduction band of Ag_3PO_4 can be separated through their

transfer to AgNPs, alwwoing a better reduction of Cr(VI). AgNPs can generate as well electrons for a direct reduction of Cr(VI) through Surface plasmon resonance (SPR) effect. Activated carbon can act as a photosensitizer to improve the visible light absorption of Ag_3PO_4 (Djellabi et al. 2022). On the other hand, the activated carbon support is able to concentrate Cr(VI) species for fast photoreduction.

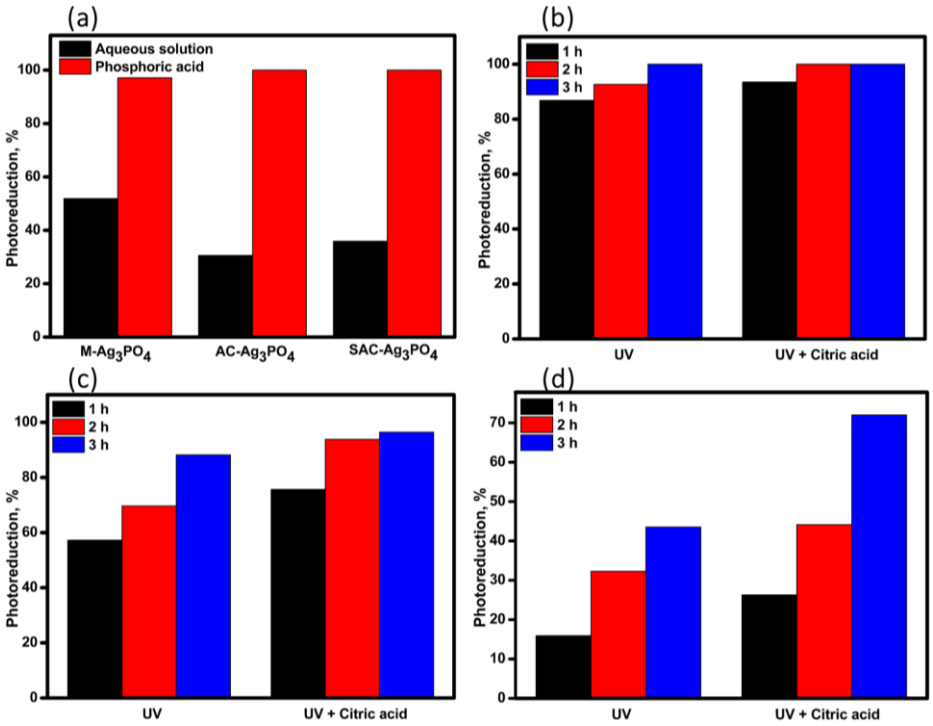

Figure 8. (a): Photoreduction of Cr(VI) by different photocatalysts under UV light without citric acid in phosphoric acid medium. [Cr(VI)]: 50 ppm, [Photocatalyst]: 1 g/L. Photoreduction of Cr(VI) at different concentrations using $SACAg_3PO_4$ under UV light with and without citric acid, (b): [Cr(VI)]: 100 ppm, (c): [Cr(VI)]: 200 ppm, (d): [Cr(VI)]: 300 ppm.

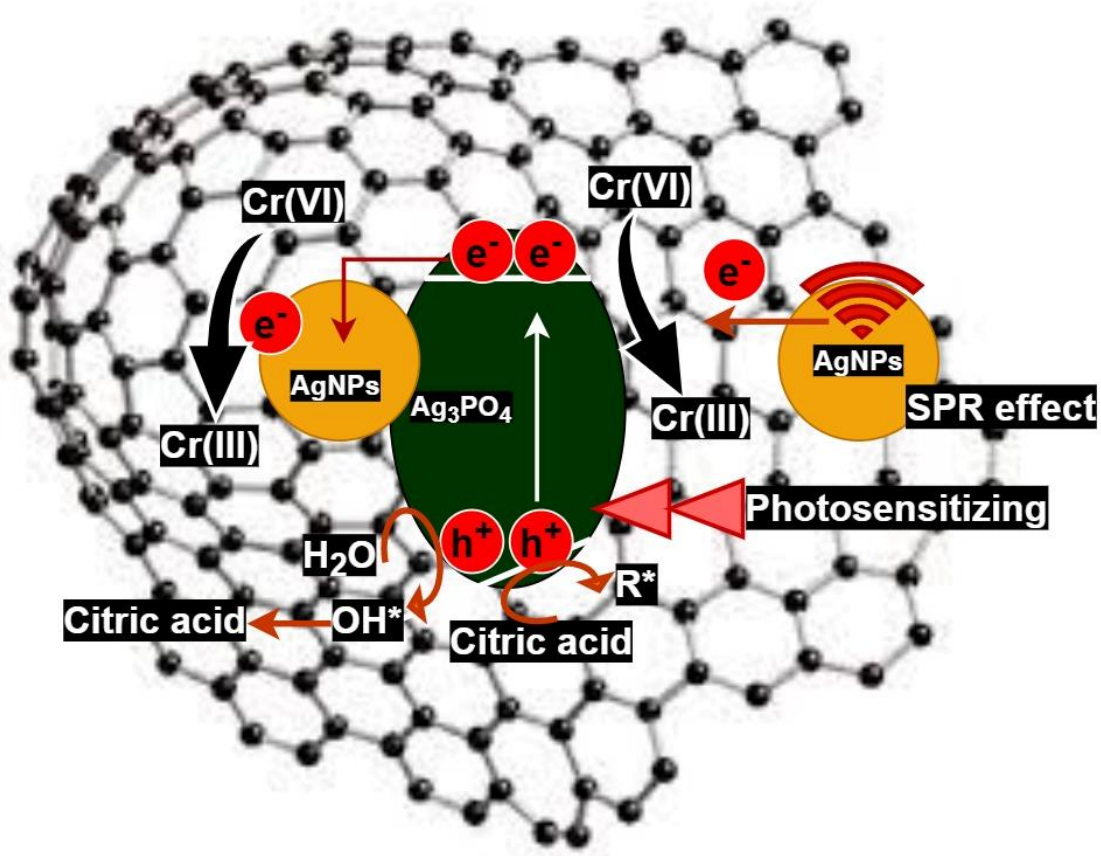

Figure 9. Simplified scheme showing the possible pathways for the photocatalytic reduction of Cr(VI) on the surface of SACAg/Ag_3PO_4.

4. Conclusions

The present study has investigated the photocatalytic reduction of Cr(VI) in water and phosphoric acid mediums using three types of as-prepared photocatalysts, namely, MAg_3PO_4, $ACAg_3PO_4$, and $SACAg_3PO_4$. Comparatively, the adsorption and photocatalytic activity were studied in aqueous solution and phosphoric acid. The addition of citric acid as a hole scavenger significantly enhanced the reduction performance in all cases. Under UV light, MAg_3PO_4 led the best photocatalytic reduction compared to the other materials. While under solar light, $SACAg_3PO_4$ and $ACAg_3PO_4$ showed enhanced photoreduction efficiency. Interestingly, the photocatalytic reduction in phosphoric acid was much faster than that in an aqueous solution. At 50 ppm of Cr(VI) in the absence of citric acid, the reduction rates were around 50, 28, and 37% for MAg_3PO_4, $ACAg_3PO_4$, and $SACAg_3PO_4$

under UV within 3 h, respectively, while in phosphoric acid medium, a total reduction was obtained by all as-prepared photocatalysts. It was claimed that the generation of ROSs in phosphoric acid would be lesser than that in an aqueous solution, which may favor the photoreduction performance. SACAg_3PO_4 showed significant reduction rates even at higher Cr(VI) concentrations (100 to 300 ppm). The results of this study are very promising in terms of the use of photocatalytic technology for the recovery of heavy metals from phosphoric acid. As a primary first investigation, this work may open the door to future research in this field to carry our further studies towards the purification of phosphoric acid produced by the wet process.

References

Abroushan, Eslam, Saeed Farhadi, and Abedien Zabardasti. 2017. 'Ag 3 PO 4/CoFe 2 O 4 magnetic nanocomposite: synthesis, characterization and applications in catalytic reduction of nitrophenols and sunlight-assisted photocatalytic degradation of organic dye pollutants', *RSC advances*, 7: 18293-304.

Ahmed, A, Y Chaker, El H Belarbi, O Abbas, JN Chotard, HB Abassi, A Nguyen Van Nhien, M El Hadri, and S Bresson. 2018. 'XRD and ATR/FTIR investigations of various montmorillonite clays modified by monocationic and dicationic imidazolium ionic liquids', *Journal of Molecular Structure*, 1173: 653-64.

Alalm, Mohamed Gar, Ridha Djellabi, Daniela Meroni, Carlo Pirola, Claudia Letizia Bianchi, and Daria Camilla Boffito. 2021. 'Toward Scaling-Up Photocatalytic Process for Multiphase Environmental Applications', *Catalysts*, 11: 562.

Amin, Mostafa Ibrahim. 2020. 'Removal of iron from wet process phosphoric acid using ion exchange method by Puromet MTS9570 resin', *International Journal of Environmental Analytical Chemistry*: 1-18.

Association, European Fertilizer Manufacturers. 2000. 'Booklet No. 4 of 8 Production of phosphoric acid', *Best Available Techniques for Pollution Prevention and Control in the European Fertilizer Industry. Accessible from: http://www. productstewardship. eu/fileadmin/user_upload/user_upload_ prodstew/documents/Booklet_nr_4_Production_of_Phosphoric_Acid. pdf (accessed June 2015) Belgium*.

Bahrpaima, Khatereh. 2017. 'Purification of Phosphoric Acid by Liquid-Liquid Equilibrium.' in, *Phosphoric Acid Industry-Problems and Solutions* (IntechOpen London).

BAI, Xi-zhu, and Shou-zhi ZENG. 2006. 'Progress of Technological Development for Phosphoric Acid Production [J]', *Sulphur Phosphorus & Bulk Materials Handling Related Engineering*, 5.

Belboom, Sandra, Carl Szöcs, and Angélique Léonard. 2015. 'Environmental impacts of phosphoric acid production using di-hemihydrate process: a Belgian case study', *Journal of Cleaner Production*, 108: 978-86.

Bianchi, Claudia Letizia, Giuseppina Cerrato, Bianca Maria Bresolin, Ridha Djellabi, and Sami Rtimi. 2020. 'Digitally printed AgNPs doped TiO2 on commercial porcelain-grès tiles: synergistic effects and continuous photocatalytic antibacterial activity', *Surfaces*, 3: 11-25.

Botelho, Gleice, Júlio César Sczancoski, Juan Andres, Lourdes Gracia, and Elson Longo. 2015. 'Experimental and theoretical study on the structure, optical properties, and growth of metallic silver nanostructures in Ag3PO4', *The Journal of Physical Chemistry C*, 119: 6293-306.

Boulkroune, N, and AH Meniai. 2012. 'Modeling purification of phosphoric acid contaminated with cadmium by liquid-liquid extraction', *Energy Procedia*, 18: 1189-98.

Chastain, Jill, and Roger C King Jr. 1992. 'Handbook of X-ray photoelectron spectroscopy', *Perkin-Elmer, USA*: 261.

Chen, Aimei, Jiawen Zhu, Kui Chen, Bin Wu, Lijun Ji, and Yanyang Wu. 2013. 'Melt suspension crystallization for purification of phosphoric acid', *Asia-Pacific Journal of Chemical Engineering*, 8: 354-61.

Chuanpin, Jin Shiwei Ouyang Yide Bao, and Chen Gusheng. 2003. 'Production of phosphoric acid and its development direction [J]', *Chemical Industry Times*, 2.

Diallo, Houda, Murielle Rabiller-Baudry, Khaoula Khaless, and Bernard Chaufer. 2013. 'On the electrostatic interactions in the transfer mechanisms of iron during nanofiltration in high concentrated phosphoric acid', *Journal of Membrane Science*, 427: 37-47.

Djellabi, R, and MF Ghorab. 2015. 'Photoreduction of toxic chromium using TiO2-immobilized under natural sunlight: effects of some hole scavengers and process parameters', *Desalination and Water Treatment*, 55: 1900-07.

Djellabi, Ridha, Mohamed Fouzi Ghorab, Abdelaziz Smara, Claudia Letizia Bianchi, Giuseppina Cerrato, Xu Zhao, and Bo Yang. 2020. 'Titania–Montmorillonite for the photocatalytic removal of contaminants from water: adsorb & shuttle process.' in, *Green materials for wastewater treatment* (Springer).

Djellabi, Ridha, Roberto Giannantonio, Ermelinda Falletta, and Claudia Letizia Bianchi. 2021. 'SWOT analysis of photocatalytic materials towards large scale environmental remediation', *Current Opinion in Chemical Engineering*, 33: 100696.

Djellabi, Ridha, Laila Noureen, Van-Duong Dao, Daniela Meroni, Ermelinda Falletta, Dionysios D Dionysiou, and Claudia L Bianchi. 2022. 'Recent advances and challenges of emerging solar-driven steam and the contribution of photocatalytic effect', *Chemical Engineering Journal*, 431: 134024.

Djellabi, Ridha, Bo Yang, Yan Wang, Xiaoqing Cui, and Xu Zhao. 2019. 'Carbonaceous biomass-titania composites with TiOC bonding bridge for efficient photocatalytic reduction of Cr (VI) under narrow visible light', *Chemical Engineering Journal*, 366: 172-80.

Djellabi, Ridha, Bo Yang, Ke Xiao, Yan Gong, Di Cao, Hafiz Muhammad Adeel Sharif, Xu Zhao, Caizhen Zhu, and Junmin Zhang. 2019. 'Unravelling the mechanistic role of TiOC bonding bridge at titania/lignocellulosic biomass interface for Cr (VI) photoreduction under visible light', *Journal of Colloid and Interface Science*, 553: 409-17.

Djellabi, Ridha, Laiqi Zhang, Bo Yang, Muhammad Rizwan Haider, and Xu Zhao. 2019. 'Sustainable self-floating lignocellulosic biomass-TiO2@ Aerogel for outdoor solar photocatalytic Cr (VI) reduction', *Separation and Purification Technology*, 229: 115830.

Djellabi, Ridha, Xu Zhao, Marcela Frias Ordonez, Ermelinda Falletta, and Claudia L Bianchi. 2021. 'Comparison of the photoactivity of several semiconductor oxides in floating aerogel and suspension systems towards the reduction of Cr (VI) under visible light', *Chemosphere*, 281: 130839.

El-Asmy, Ahmed A, Homam M Serag, Mohammad A Mahdy, and Moustafa I Amin. 2008. 'Purification of phosphoric acid by minimizing iron, copper, cadmium and fluoride', *Separation and Purification Technology*, 61: 287-92.

El-Zahhar, AA, SEA Sharaf El-Deen, and RR Sheha. 2013. 'Sorption of iron from phosphoric acid solution using polyacrylamide grafted activated carbon', *Journal of Environmental Chemical Engineering*, 1: 290-99.

Khaless, Khaoula, Brahim Achiou, Rachid Boulif, and Rachid Benhida. 2021. 'Recycling of Spent Reverse Osmosis Membranes for Second Use in the Clarification of Wet-Process Phosphoric Acid', *Minerals*, 11: 637.

Kijkowska, R, D Pawlowska-Kozinska, Z Kowalski, M Jodko, and Z Wzorek. 2002. 'Wet-process phosphoric acid obtained from Kola apatite. Purification from sulphates, fluorine, and metals', *Separation and Purification Technology*, 28: 197-205.

Kloprogge, JT. 2017. 'Infrared and Raman Spectroscopies of Clay Minerals.' in, *Developments in Clay Science, Volume 8* (Elsevier, Amsterdam).

Kouzbour, Sanaa, Bouchaib Gourich, Fabrice Gros, Christophe Vial, Fouad Allam, and Youssef Stiriba. 2019. 'Comparative analysis of industrial processes for cadmium removal from phosphoric acid: A review', *Hydrometallurgy*, 188: 222-47.

Loeb, Stephanie K, Pedro JJ Alvarez, Jonathon A Brame, Ezra L Cates, Wonyong Choi, John Crittenden, Dionysios D Dionysiou, Qilin Li, Gianluca Li-Puma, and Xie Quan. 2018. "The technology horizon for photocatalytic water treatment: sunrise or sunset?" In.: ACS Publications.

Ma, Chao, Yuan-xin Wu, Fang Jin, Xi LI, and Biao HU. 2013. 'Current status and prospect of industrial phosphoric acid production [J]', *Chemical Engineering (China)*, 6.

Ma, Jinling, Xiaojun Niu, Jie Wang, and Jiandong Wu. 2016. 'Facile synthesis of Ag3PO4 with the assistance of N, N-dimethylformamid and urea for high performance photocatalysis', *Catalysis Communications*, 77: 55-59.

Marinho, Belisa A, Raquel O Cristóvão, Ridha Djellabi, José M Loureiro, Rui AR Boaventura, and Vítor JP Vilar. 2017. 'Photocatalytic reduction of Cr (VI) over TiO2-coated cellulose acetate monolithic structures using solar light', *Applied Catalysis B: Environmental*, 203: 18-30.

Naciri, Y, A Hsini, A Bouziani, R Djellabi, Z Ajmal, M Laabd, JA Navío, A Mills, CL Bianchi, and H Li. 2021. 'Photocatalytic oxidation of pollutants in gas-phase via Ag3PO4-based semiconductor photocatalysts: Recent progress, new trends, and future perspectives', *Critical Reviews in Environmental Science and Technology*: 1-44.

Nasr, Bensalah, Benamor Hedi, Gadri Abdellatif, and Manuel A Rodrigo. 2005. 'Purification of Wet-Process Phosphoric Acid by Hydrogen Peroxide Oxidation, Activated Carbon Adsorption and Electrooxidation', *Chemical Engineering & Technology: Industrial Chemistry-Plant Equipment-Process Engineering-Biotechnology*, 28: 193-98.

Saber, Ayman N, Ridha Djellabi, Imen Fellah, Nesrine Abderrahim, and Claudia L Bianchi. 2021. 'Synergistic sorption/photo-Fenton removal of typical substituted and parent polycyclic aromatic hydrocarbons from coking wastewater over CuO-Montmorillonite', *Journal of Water Process Engineering*, 44: 102377.

Tang, Cong, Yi Qiu, Ye Wang, Xinlong Wang, Zhiye Zhang, and Lin Yang. 2018. 'Kinetic studies on Al3+ removal from phosphoric acid by cation exchange resin', *The Canadian Journal of Chemical Engineering*, 96: 944-54.

Trench, Aline Barrios, Thales Rafael Machado, Amanda Fernandes Gouveia, Marcelo Assis, Leticia Guerreiro da Trindade, Clayane Santos, Andre Perrin, Christiane Perrin, Monica Oliva, and Juan Andres. 2018. 'Connecting structural, optical, and electronic properties and

photocatalytic activity of Ag3PO4: Mo complemented by DFT calculations', *Applied Catalysis B: Environmental*, 238: 198-211.

Wan, Jun, Enzhou Liu, Jun Fan, Xiaoyun Hu, Lin Sun, Chunni Tang, Yunchao Yin, Hua Li, and Yang Hu. 2015. 'In-situ synthesis of plasmonic Ag/Ag3PO4 tetrahedron with exposed {111} facets for high visible-light photocatalytic activity and stability', *Ceramics International*, 41: 6933-40.

Wu, Shengxi, Liangshi Wang, Patrick Zhang, Hassan El-Shall, Brij Moudgil, Xiaowei Huang, Longsheng Zhao, Lifeng Zhang, and Zongyu Feng. 2018. 'Simultaneous recovery of rare earths and uranium from wet process phosphoric acid using solvent extraction with D2EHPA', *Hydrometallurgy*, 175: 109-16.

ZHANG, Lichang, CHEN Qianlin, KANG Chao, MA Xin, and YANG Zunliang. 2016. 'Rare earth extraction from wet process phosphoric acid by emulsion liquid membrane', *Journal of rare earths*, 34: 717-23.

Zhong, Qin, Tao Luo, Zhengjuan Yan, Lin Yang, Zhiye Zhang, and Xinlong Wang. 2021. 'Purification of Wet-Process Phosphoric Acid via Donnan Dialysis with a Perfluorinated Sulfonic Acid Cation-Exchange Membrane', *Membranes*, 11: 298.

Zhou, Li, Oscar González Alvarez, Carmen Sans Mazon, Ling Chen, Huiping Deng, and Minghao Sui. 2016. 'The roles of conjugations of graphene and Ag in Ag 3 PO 4-based photocatalysts for degradation of sulfamethoxazole', *Catalysis Science & Technology*, 6: 5972-81.